7 April 1995

ELSEVIER

Chemical Physics Letters 236 (1995) 37–42

CHEMICAL PHYSICS LETTERS

Calculated paramagnetic properties of matrix isolated Au_3 cluster

Ramiro Arratia-Pérez [a,*], Lucía Hernández-Acevedo [a], Juan S. Gómez-Jeria [b]

[a] *Kent 9461, Villa el Inglés, La Florida, Santiago, Chile*

[b] *Facultad de Ciencias, Universidad de Chile, Casilla 653, Santiago, Chile*

Received 30 January 1995

Abstract

Non-relativistic (NR-Xα) and Dirac (DSW-Xα) spin-restricted calculations on the matrix isolated Au_3 cluster are reported. It is shown that the resolved hyperfine interactions arising from the apical gold atom and the anisotropic effects on the spin distribution and on the paramagnetic properties could be adequately interpreted by using Dirac operators and Dirac cluster wave functions. The DSW-Xα calculations are in reasonable agreement with empirical and resolved paramagnetic resonance data of the Au_3 cluster isolated on the C_6D_6 matrix.

1. Introduction

It is now recognized that electronic paramagnetic resonance (EPR) spectroscopy has been useful in elucidating cluster electronic structure, possible cluster geometries, electronic states and spin distributions [1–5]. Furthermore, highly resolved EPR spectra of heavy-metal cluster radicals give detailed information about the isotropic and anisotropic character of the magnetic tensors [6,7].

About a decade ago, the EPR spectrum of the matrix isolated Au_3 cluster was reported [8]. It was concluded that the spectrum arises from a single unpaired electron which shows equal, large, almost isotropic hyperfine interaction (hfi), with two equivalent Au atoms and a further, small interaction with a third Au atom [4,8]. Moreover, this species was empirically characterized as having an obtuse angled geometry with a $^2B_2$ electronic ground state [4,8].

From a theoretical point of view the electronic structure and the molecular stabilities of the Au_3 cluster have been the subject of several nonrelativistic (NR) Schrödinger or Pauli-type theoretical studies [9–13]. The NR semiempirical diatomics in molecules calculation predicts a cluster with an acute angled geometry with a $^2A_1$ ground state [9]. However, the Pauli-type MRSDCI calculations by Balasubramanian et al. [10–12], and the NR-SDCI calculations by Bauschlicher [13], predicted the $^2B_2$ (C_{2v}) electronic obtuse ground state as the bent minima, which is nearly degenerate with the low-lying $^2A_1$ (C_{2v}) acute excited state [10–13]. This prediction is more in accord with the EPR interpretation [4,8].

In the present study, we examine the role of relativistic effects (including spin–orbit interaction) on the spin populations and paramagnetic properties of the obtuse Au_3 cluster. We report here nonrelativistic and relativistic spin populations and paramagnetic tensor calculations by using the methods previously developed by us [14–16]. We have recently shown that for extracting meaningful informa-

* Corresponding author.

SSDI 0009-2614(95)00000-0

tion from the EPR spectra of heavy-atom clusters, certainly requires the use of Dirac type operators and orbitals [16].

2. Method of calculations

In the self-consistent NR-Xα and DSW-Xα formalisms the molecular wave function is approximated as a Slater determinant by an effective Coulomb and exchange–correlation potential [17]. For the exchange–correlation potential we used the Hedin–Lundqvist local density potential [18], modified according to MacDonald and Vosko [19] to include relativistic effects [16,19]. The calculation of the molecular hyperfine interaction uses the SCF NR-Xα or Dirac molecular wave function as the starting point.

In relativistic theory the method used for the calculation of the magnetic hyperfine interactions is based upon a first-order perturbation to the Dirac Hamiltonian, so that the effects of magnetic fields are described by the perturbation operator H_D [14–17], where

$$H_D = e\boldsymbol{\alpha} \cdot \boldsymbol{A} \qquad (1)$$

In Eq. (1), $\boldsymbol{\alpha}$ is the vector of 4×4 Dirac matrices and $\boldsymbol{A}$ is the electromagnetic vector potential. For the hfi term $\boldsymbol{A} = (\boldsymbol{\mu} \times \boldsymbol{r})/r^3$, where $\boldsymbol{\mu}$ is the nuclear magnetic dipole moment. For the Zeeman term $\boldsymbol{A} = \frac{1}{2}(\boldsymbol{B} \times \boldsymbol{r})$, where $\boldsymbol{B}$ is the external magnetic field. At the nonrelativistic limit ($c \to \infty$) Eq. (1) reduces to the usual nonrelativistic magnetic operators [1].

The resulting perturbation energies are then fitted to the spin Hamiltonian

$$H_n = \boldsymbol{I}_n \cdot \mathbf{A}_n \cdot \boldsymbol{S} + \boldsymbol{S}' \cdot \mathbf{g} \cdot \boldsymbol{B}, \qquad (2)$$

where a value of $S = 1/2$ is used to describe the ground state Kramer doublet, $\boldsymbol{I}_n$ is a nuclear spin operator, and n denotes the apical Au(1) and terminal Au(2) atoms, $\mathbf{A}_n$ and $\mathbf{g}$ are its associated hyperfine and Zeeman tensors, respectively [15].

The Au(1)–Au(2) bond distances $d = 2.60$ Å and the apex bond angle $\theta = 65.7°$ for Au_3 were adopted from the MRSDCI calculations, since these included two-component spin–orbit correlated functions which are important for clusters containing heavy atoms [10–12].

3. Results and discussion

The calculated total valence populations of Au_3 are given in Table 1. These are reported in terms of the atomic like spinors as calculated by a relativistic (and its nonrelativistic limit) population analysis algorithm [14,17], and are also given in terms of a Mulliken gross populations analysis, as calculated by the MRSDCI method [10–12]. These calculations suggest that the formal atomic charges for Au_3 ($^2B_2$) could be assigned as indicated (see footnote c in Table 1). Interestingly, the three methods predict that the apical gold atom carries the positive charge, thus giving rise to a positive dipole moment for Au_3 [10]. We should bear in mind, however, that the MRSDCI method is a two-component Pauli-type calculation [10–12], while the DSW-Xα is a four-vector Dirac-type calculation which reduces to a one-component Schrödinger-type calculation at its nonrelativistic limit (NR-Xα) [14–17]. Nevertheless, the agreement

Table 1
Total valence populations of Au_3

Atom	κ [a]	j	Obtuse NR	Obtuse DSW-Xα	MRSDCI
Au(1)	−1	1/2	0.669	0.838	0.741
	1	1/2	0.128	0.160	
	−2	3/2	0.255	0.165	
	total p		0.383	0.325	0.147
	2	3/2	3.903	3.839	
	−3	5/2	5.854	5.764	
	total d		9.757	9.603	9.950
	total Au(1)		10.809	10.766	10.838
Au(2)	−1	1/2	0.991	1.111	1.084
	1	1/2	0.095	0.130	
	−2	3/2	0.190	0.138	
	total p		0.285	0.268	0.113
	2	3/2	3.928	3.904	
	−3	5/2	5.891	5.834	
	total d		9.819	9.738	9.885
	total Au(2)		11.095	11.117	11.081

[a] The κ quantum defines both l and j through $\kappa = -a(j + 1/2)$ with $a = 1$ for $j = l + 1/2$ and $a = -1$ for $j = l - 1/2$.
[b] Mulliken gross populations analysis, see Ref. [10].
[c] Calculated charge distributions: DSW-Xα: $Au^{+0.234}Au_2^{-0.117}$, NR-Xα: $Au^{+0.19}Au_2^{-0.095}$, MRSDCI: $Au^{+0.162}Au_2^{-0.081}$.

Table 2
Spin populations (SOMO)

(a) in terms of atomic spinors

Atom	Spinor	DSW	NR
Au(1)	$s_{1/2}$	0.043	– [a]
	$p_{1/2}$	0.054	0.046
	$p_{3/2}$	0.029	0.094
	total p	0.083	0.148
	$d_{3/2}$	0.023	0.011
	$d_{5/2}$	0.055	0.017
	total d	0.078	0.028
Au(2)	$s_{1/2}$	0.318	0.347
	$p_{1/2}$	0.039	0.020
	$p_{3/2}$	0.017	0.041
	total p	0.056	0.061
	$d_{3/2}$	0.012	0.003
	$d_{5/2}$	0.012	0.005
	total d	0.024	0.008

(b) in terms of Pauli decomposition

Atom	l	m	DSW α	DSW β	NR α	NR β
Au(1)	0	0	– [a]	0.043	–	–
	1	−1	0.049	–	0.070	–
	1	0	–	0.008	–	–
	1	1	0.026	–	0.070	–
	2	−1	0.036	–	0.014	–
	2	0	–	0.000	–	–
	2	1	0.041	–	0.014	–
	2	2	–	0.001	–	–
	2	−2	–	0.000	–	–
Au(2)	0	0	0.306	0.012	0.347	–
	1	−1	0.032	0.000	0.029	–
	1	0	0.000	0.008	0.002	–
	1	1	0.016	0.000	0.029	–
	2	−1	0.000	0.000	0.000	–
	2	0	0.002	0.002	0.003	–
	2	1	0.000	0.000	0.000	–
	2	2	0.010	0.001	0.003	–
	2	−2	0.008	0.001	0.003	–
total MO			0.900	0.100	1.000	–

[a] Dashes indicate contributions forbidden by single point group symmetry.

between these calculational approaches to cluster electronic structure is meaningful.

In the present NR-Xα and DSW-Xα spin restricted calculations, all the cluster spin densities arise from the single occupied molecular orbital (SOMO). Table 2 gives the calculated spin populations for Au_3. These are given in terms of atomic-like spinor for $j = 1/2$, $3/2$ and $5/2$, and are also reported in terms of a Pauli description consisting of spherical harmonics multiplied by spin functions. In the latter procedure we consider only the two 'large' components of the relativistic wave functions and assume that the radial wave functions are the same for $j = l + 1/2$ and $j = l - 1/2$. The sum of such Pauli spinors can be interpreted as nonrelativistic functions of mixed spin [16]. In the nonrelativistic limit the ratio of populations for $j = l + 1/2$ to $j = l - 1/2$ is required to be $(l+1)/l$ (for $l > 0$) [15,17].

One measure of the extent of spin–orbit mixing into the relativistic SOMO is to determine the amount of minority spin from the Pauli decomposition scheme (see Table 2). The SOMO level contains small but nonnegligible amounts of minority spin, 11% of β spin, which is larger than the minority spin (2.5% β) of the corresponding obtuse Ag_3 cluster [16]. This is expected, since the gold orbitals are more affected than the silver orbitals due to relativistic effects. We shall see later, that the origin of these spin contaminations are mostly due to isotropic charge contributions.

Moreover, the calculated relativistic SOMO–LUMO gap for Au_3 amounts to 0.51 eV, while a value of 0.21 eV was calculated for the obtuse Ag_3 cluster [16]. Then, applying the principles of density functional theory [21,22], the obtuse Au_3 cluster would be harder than the corresponding obtuse Ag_3 cluster, and than the acute Ag_3 cluster [16]. This argument is consistent with the fact that both obtuse Ag_3 and Au_3 clusters were isolated on the C_6D_6 matrix, while the less stable acute Ag_3 cluster was only isolated on the N_2 matrix [3–5]. To our knowledge there are no reports of the isolation of the acute Au_3 cluster on a different matrix. Obviously, matrix effects will tend to distort the softer cluster [16]. Therefore, the relative softness variation is S: Ag_3 ($^2A_1$) > Ag_3 ($^2B_2$) > Au_3 ($^2B_2$).

3.1. Spin populations

As shown in Table 2, the larger relativistic and nonrelativistic spin populations for Au_3 correspond to the $6s_{1/2}$ (31.8%) and 6s (34.7%) spinors for the terminal Au(2) atoms. It should be noticed that 6s contributions for the apical Au(1) atom is forbidden

by single point symmetry, but in relativistic theory these $6s_{1/2}$ contributions (4.3%) are allowed by double point group symmetry. This interpretation is in agreement with the small resolved hyperfine interaction of Au(1) [4,8].

We shall bear in mind that in Dirac and Pauli theory the charge distribution arising from $j = 1/2$ (either $s_{1/2}$ or $p_{1/2}$) is spherically symmetric, and its contributions to the magnetic interactions is isotropic. Similarly, the contributions from $j = 3/2$ or $5/2$ states will give rise to anisotropic magnetic interactions since these charge distributions are nonspherical [15,16]. Applying these concepts, we can estimate the relativistic isotropic ($\rho_{iso} = \rho_{6s_{1/2}} + \rho_{6p_{1/2}}$) and the relativistic anisotropic ($\rho_{aniso} = \rho_{6p_{3/2}} + \rho_{5d_{3/2}} + \rho_{5d_{3/2}}$) spin populations for Au_3. In the nonrelativistic limit these spin distributions are usually defined like $\rho_{iso} = \rho_{6s}$ and $\rho_{aniso} = \rho_{6p} + \rho_{5d}$ [1,4,8].

The calculated total NR and relativistic isotropic spin populations for the Au_3 cluster can be extracted from Table 3, and recognizing that for a total unit spin population should obey $\rho_{Au_3} = \rho_{Au(1)} + 2\rho_{Au(2)}$ [1–4,8].

Then, the isotropic spin population are 0.694 and 0.811 as calculated by the NR-Xα and DSW-Xα approaches, and the value of 0.9 was empirically deduced by EPR [8]. The relativistically calculated (0.811) and the empirical resolved (0.9) spin populations are in reasonable agreement, but it should be noticed that the empirical estimate was obtained from the ratio between the observed cluster hfi and the atomic gas-phase hfi [4,8]. Therefore, the empirical model neglects orbital deformation effects due to cluster bond formation.

Table 3
Isotropic and anisotropic spin populations

		Au(1)	Au(2)	ρ_{total}
ρ_{iso}	NR-Xα	– [a]	0.347	0.694
	DSW-Xα	0.097	0.357	0.811
	empirical [b]	~ 0.060	~ 0.420	~ 0.900
ρ_{aniso}	NR-Xα	0.168	0.069	0.306
	DSW-Xα	0.107	0.041	0.189
	empirical [b]			~ 0.100 [c]

[a] Forbidden by single point group symmetry.
[b] Empirically estimated by EPR, see Refs. [4] and [8].
[c] Assumed value to comply with a unit spin population, see Ref. [8] and text.

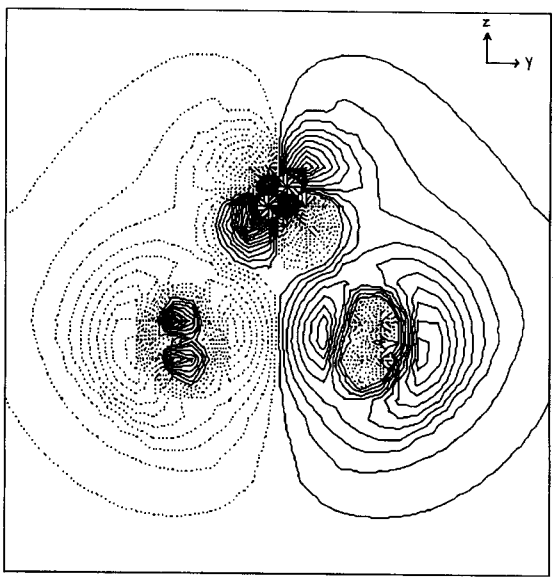

Fig. 1. Contours of the largest component (Ψ_1) of the SOMO of Au_3 in the yz plane. Contour values (electron/bohr^3)$^{1/2}$ are between +0.2124 and −0.2124 with increments of 0.0109. Negative contours are plotted as dashed lines.

The anisotropic spin population as calculated nonrelativistically and relativistically are 0.306 and 0.189, respectively. Since the total resolved spin population should be close to 1.0, the empirical analysis assigned the remaining anisotropic spin population in terms of nonrelativistic orbitals $\rho_{5d,6p}$ to be near to 0.10 [4,8]. Thus, the associated relativistically calculated and empirical anisotropic spin populations are in close agreement, but keeping in mind that the empirical model neglects the small anisotropic contributions arising from the apical Au(1) atom. These results would imply that, if the EPR spectrum of the Au_3 cluster were recorded at 4.2 K, it should show larger anisotropies than the obtuse Ag_3 cluster [16].

In order to get a visual picture of the SOMO, we plotted the largest component of the relativistic wave function contours, which is shown in Fig. 1. The antibonding character of the SOMO is clearly seen and possess global π symmetry, characteristic for a $^2B_2$ ground state. There is more d character mixed in the SOMO of Au_3, than the corresponding SOMO of Ag_3 [16].

Table 4
Hyperfine coupling constants (in G) of Au_3

		$A_{\parallel}$	$A_{\perp}$	a_{iso} [b]
^{197}Au(1)	NR calc.	1.8	3.8	– [c]
	DSW calc.	70.2	47.8	60.3
	expt. [a,b]	–	–	58.0
^{197}Au(2)	NR calc.	167.8	170.4	168.5
	DSW calc.	400.5	415.6	408.3
	expt. [a,b]	–	–	382.9

[a] See Refs. [4] and [8].
[b] Reported as the isotropic part of the cluster hfi.
[c] Forbidden by single point group symmetry.

3.2. Magnetic interactions

The calculated and experimental hyperfine coupling constants for gold trimer are listed in Table 4. It can be seen that the DSW-Xα calculated isotropic constant for the apical gold atom is in good agreement with the experimental value. However, this isotropic contribution to the total hyperfine tensor is forbidden by nonrelativistic symmetry (see Table 4). Thus, the observed isotropic contribution of the apical Au(1) atom could be only interpreted in terms of Dirac molecular orbital theory. It could be noted that the DSW-Xα calculation predicts anisotropic magnetic behavior, since $A_{\parallel} - A_{\perp} \neq 0$.

The DSW-Xα and the experimental hfi tensors for the basal Au(2) atoms are in fairly good agreement, but the NR-Xα value is far away from the resolved value. However, both calculational approaches predict anisotropic behavior. The calculated anisotropies of the magnetic hyperfine tensors for both, the apical Au(1) and the basal Au(2) atoms, are of about 15 G, which can certainly be observed by high resolution EPR spectroscopy [6,7]. Moreover, the experimental isotropic negative g shift, $\Delta g_{exp} = -0.1373$ agrees with the calculated value of $\Delta g_{calc} = -0.1497$. This large negative isotropic Δg suggests that the unpaired electron in the $^2B_2$ state acquires orbital angular momentum by coupling with the low-lying $^2A_1$ state.

4. Conclusions

In this study we have shown that the application of nonrelativistic theories is not appropriate for describing magnetic behavior of heavy-metal clusters. Also, we have shown that Pauli-type and Dirac-type calculations could properly describe isotropic and anisotropic spin populations. However, only the application of Dirac wave functions and Dirac operators could adequately describe the magnetic behavior of heavy cluster radicals since the large and small components of the cluster wave function are coupled together in the relativistic perturbational Hamiltonian describing magnetic interactions (see Eq. (1)).

Acknowledgement

We thank J. Pablo Bravo-Vasquez for assistance with part of the calculations. This work was supported by Fondecyt and the Comission of the European Communities (Contract CI1-CT93-0330CL).

References

[1] W. Weltner Jr., in: Magnetic atoms and molecules (Van Nostrand, New York, 1983).
[2] W. Weltner Jr. and R.J. Van Zee, Ann. Rev. Phys. Chem. 35 (1984) 291.
[3] J.A. Howard, K.F. Preston and B. Mille, J. Am. Chem. Soc. 103 (1981) 6226.
[4] J.A. Howard, R. Sutcliffe and B. Mille, Surface Sci. 156 (1985) 214.
[5] K. Kernisant, G.A. Thompson and D.M. Lindsay, J. Chem. Phys. 82 (1985) 4739.
[6] A. van der Pool, E.J. Reijerse and E. de Boer, Mol. Phys. 75 (1992) 37.
[7] J. Michalik, T. Wasowicz, A. van der Pol, E.J. Reijerse and E. de Boer, J. Chem. Soc. Chem. Commun. (1992) 29.
[8] J.A. Howard, R. Sutcliffe and B. Mile, J. Chem. Soc. Chem. Commun. (1983) 1449.
[9] S.C. Richtsmeier, J.L. Gole and D.A. Dixon, Proc. Natl. Acad. Sci. USA 77 (1980) 5611.
[10] K. Balasubramian and M.Z. Liao, Chem. Phys. 127 (1988) 313.
[11] K. Balasubramanian and M.Z. Liao, J. Chem. Phys. 86 (1987) 5587.
[12] K. Balasubramanian and K.K. Das, Chem. Phys. Letters 186 (1991) 577.
[13] C.W. Bauschlicher Jr., Chem. Phys. Letters 156 (1989) 91.
[14] R. Arratia-Pérez and D.A. Case, J. Chem. Phys. 79 (1983) 4939.
[15] R. Arratia-Pérez and G.L. Malli, J. Magn. Reson. 73 (1987) 134.
[16] J. Pablo Bravo-Vásquez and R. Arratia-Pérez, J. Phys. Chem. 98 (1994) 5627.

[17] C.Y. Yang and D.A. Case, in: Local density approximations in quantum chemistry and solid state physics, eds. J.P. Dahl and J. Avery (Plenum Press, New York, 1983).
[18] L. Hedin and B.I. Lundqvist, J. Phys. C 4 (1974) 2064.
[19] A.H. MacDonald and S.H. Vosko, J. Phys. C 12 (1979) 2977.
[20] M.P. Das, M.V. Ramana and A.K. Rajagopal, Phys. Rev. A 22 (1980) 9.
[21] R.G. Parr and Z. Zhou, Accounts Chem. Res. 26 (1993) 256.
[22] W. Yang and R.G. Parr, Proc. Natl. Acad. Sci. USA 82 (1985) 6723.